Lunar Dust Levitation

Joshua E. Colwell[1]; Scott R. Robertson[2]; Mihály Horányi[3]; Xu Wang[4]; Andrew Poppe[5]; and Patrick Wheeler[6]

Abstract: Observations of a lunar "horizon glow" by several Surveyor spacecraft on the lunar surface in the 1960s and detections of dust particle impacts by the Apollo 17 Lunar Ejecta and Meteoroid Experiment have been explained as the result of micron-sized charged particles lifting off the surface. The surface of the Moon is exposed to the solar wind and solar UV radiation causing photoemission, so it develops a surface charge and an electric field near the surface. Dust particles injected into this plasma from the lunar regolith, whether from human and mechanical activity or from meteoroid impacts or electrostatic forces, may be stably levitated above the surface and may undergo preferential deposition onto areas of the lunar surface (or equipment) with different electrical properties. This can lead to a net transport as well as contamination of sensitive equipment. This paper reports on new experimental measurements and numerical simulations of the plasma environment above the lunar surface and the related behavior of charged dust.

DOI: 10.1061/(ASCE)0893-1321(2009)22:1(2)

CE Database subject headings: Moon; Dust; Spacecraft; Space exploration.

Introduction

The lunar regolith consists of a broad size distribution of particles created by bombardment of the Moon by interplanetary debris. The smallest particles in the regolith are particularly susceptible to nongravitational forces. Under conditions which are expected to be quite common, a local electric field near the lunar surface can act to counter gravity and lift micron-sized particles off the surface. This charged dust transport has been proposed for asteroids as well as for the Moon (e.g. Pelizzari and Criswell 1978; Lee 1996; Nitter et al. 1998; Colwell et al. 2005; Stubbs et al. 2006). These particles may immediately reimpact the surface following a nearly ballistic trajectory, or they may spend an extended period of time above the surface if the electric and gravitational forces balance. Submicron-sized particles may be accelerated to velocities allowing them to reach 10^2–10^3 m in altitude or even escape the Moon's gravity altogether. Launching from the surface by electrostatic forces depends on the local surface charge, which in turn depends on the exposure of the surface to charging currents, such as sunlight and the solar wind. Thus, there can be a transport of dust on both small and large spatial scales. Future manned and unmanned activities on the lunar surface will have to contend with the contamination hazard posed by small, charged lunar regolith particles.

Lacking an atmosphere to shield its surface from high energy solar radiation and the solar wind, the surface of the Moon charges to an equilibrium potential determined by the local charging currents. The charging currents on the lunar surface are photoemission of electrons, collection of solar wind electrons and solar wind ions, and secondary electron emission in the case of energetic electrons from the Earth's magnetosphere hitting the Moon (Colwell et al. 2007). The net result is a positive charge on the dayside where photoemission dominates and a negative charge on the nightside where collection of solar wind electrons dominates. The individual particles on the surface will have a range of charges as contact charging (due to differences in the work functions of particles or mineral grains within particles) and triboelectric charging (due to friction between particles) introduce variations in the charges of individual particles (Sternovsky et al. 2002).

The charging of isolated particles in plasma sheaths and photoelectron sheaths has been studied experimentally and agrees with models (e.g., Sickafoose et al. 2000, 2001). These experiments show that the charge of a particle scales linearly with particle radius for the sizes considered here ["dust" refers to particles smaller than 100 μm, following Colwell et al. (2007) though most observations and models of levitated lunar dust concern particles between 0.1 and 10 μm; narrower size ranges are specified in the following where applicable]. Recent experimental work has studied the charge of individual dust particles on a variety of surfaces under a plasma similar to the lunar nightside (Wang et al. 2007). Experimental studies have also shown that dust particles can be levitated in a plasma sheath such as would be found on the lunar nightside (Doe et al. 1994; Arnas et al. 1999; Sickafoose et al. 2002; Robertson et al. 2003). This paper reports on experimental studies of horizontal dust transport in a plasma. It is find that the dust redistributes itself to minimize gradients in the electrostatic surface potential. However, the details of the dust trans-

[1]Dept. of Physics, Univ. of Central Florida, Orlando, FL 32816-2385. E-mail: jcolwell@physics.ucf.edu

[2]Dept. of Physics, Univ. of Colorado, 390 UCB, Boulder, CO 80309-0390.

[3]Laboratory for Atmospheric and Space Physics, Univ. of Colorado, 392 UCB, Boulder, CO 80309-0392.

[4]Dept. of Physics, Univ. of Colorado, 390 UCB, Boulder, CO 80309-0390.

[5]Dept. of Physics, Univ. of Colorado, 390 UCB, Boulder, CO 80309-0390.

[6]Dept. of Physics, Univ. of Colorado, 390 UCB, Boulder, CO 80309-0390.

Note. Discussion open until June 1, 2009. Separate discussions must be submitted for individual papers. The manuscript for this paper was submitted for review and possible publication on June 19, 2006; approved on February 28, 2007. This paper is part of the ***Journal of Aerospace Engineering***, Vol. 22, No. 1, January 1, 2009. ©ASCE, ISSN 0893-1321/2009/1-2–9/$25.00.

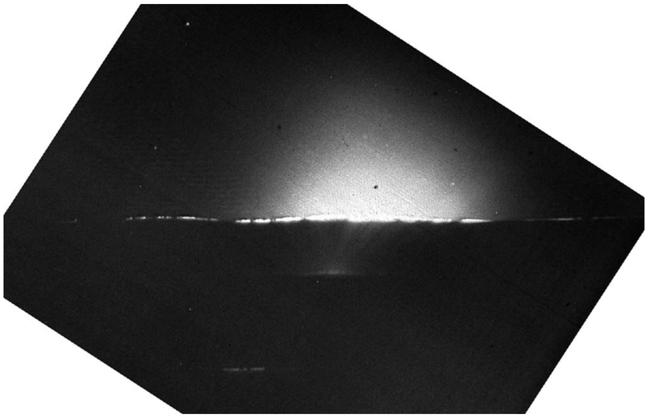

Fig. 1. Surveyor 6 image 328141526.354 showing a glow on the western lunar horizon after sunset. The broad and high diffuse glow is zodiacal light from interplanetary dust. The low bright band just at the horizon is lunar "Horizon Glow" apparently due to light scattered from dust particles near the lunar surface. National Space Science Data Center.

port depend also on the mechanical properties of the dust, with tightly packed dust exhibiting different behavior than loosely packed dust. Experimental results on near-surface electric fields are presented in this paper following a brief review of the observational evidence for charged dust dynamics near the lunar surface.

The problem of lunar dust levitation conditions has been studied theoretically and numerically and is reviewed in Colwell et al. (2007). Particle levitation is made possible by the gradient in the plasma properties near the surface producing a near-surface electric field. The variation of the electric field strength with distance from the surface depends on the distribution of electrons and ions in this sheath region. Analytic solutions for idealized electron energy distributions for a one-dimensional photoelectron sheath (Grard and Tunaley 1971) have been used to calculate electric field strengths as well as charging currents to particles in the sheath (e.g., Colwell et al. 2005; 2007). Particle-in-cell calculations of the vertical distribution of electron densities in a photoelectron sheath are presented and copared to the standard analytic solution. Results of simulations of the dynamics of charged grains above the lunar surface for different conditions and locations on the Moon are also presented.

Observations

Direct observations of dust above the lunar surface were made by the Surveyor 5, 6, and 7 spacecraft (Rennilson and Criswell 1974); Fig. 1. Apollo 17 astronauts in the orbiting command module reported and sketched high altitude streamers that have been attributed to dust leaving the lunar surface at high speeds (McCoy and Criswell 1974; Zook and McCoy 1991; Stubbs et al. 2006). The star-tracker camera on the Clementine spacecraft also imaged a glow along the lunar horizon that may be due to levitated lunar dust (Zook et al. 1995). The Lunar Ejecta And Meteorites Experiment (LEAM) deployed on the surface by the crew of Apollo 17 showed evidence for lunar regolith dust particles moving over the surface with enhanced activity near sunrise and sunset (Berg et al. 1973; 1976; see also Colwell et al. 2007). Taken together these observations argue for levitation of dust from the lunar regolith above the lunar surface with peak activity occurring near sunrise and sunset where strong terminator electric fields are predicted (Criswell 1974; Criswell and De 1977; De and Criswell 1977). At the terminator, particularly strong local electric fields (1 kV/m, over a spatial scale of 1 cm or less) can be generated at shadow boundaries due to photoelectron emission from the unevenly illuminated surfaces.

Apollo astronauts placed lunar laser reflectors on the lunar surface to measure the distance to the Moon with high (millimeter) precision (Bender et al. 1973). The fact that all of these reflector arrays (Apollo 11, 14, and 15, and Lunokhod 2) still perform without any increased attenuation of the return signal is a possible counterargument for the effects of lunar dust levitation and transport. However, these reflectors are made of glass corner-cube arrays and may have continued to perform due to their slanted smooth surfaces (the arrays are placed on a slanted platform), or due to their similar electrostatic charging properties as the glassy lunar soil. The experiments described in the following show that dust redistributes itself to minimize gradients in surface potential, and the reflector surfaces, being glass like the regolith, may charge to a potential similar to the lunar surface. A thin veneer of submicron dust particles also may not render the reflectors unusable.

There is still much that is unknown about the conditions that lead to charged dust activity on the Moon. Observational limits on the prevalence and magnitude of charged dust transport can be placed by noting the static nature of the lunar regolith during and between manned and unmanned visits. Thirty-one months after the Surveyor 3 spacecraft landed on the Moon the Apollo 12 astronauts visited the spacecraft and returned pieces of the spacecraft and photographs of the area near the Surveyor (Fig. 2). Although dust was clearly deposited on the mirror of Surveyor 3's television camera system, this may have been deposited during the landing of Surveyor 3 (or by the Apollo 12 Lunar Module 155 m away) when its engine blew dust off the lunar surface. (Indeed, this is another significant potential dust hazard for future missions.) There are no measurements of the amount of dust on the rest of the spacecraft and no way to determine if the distribution of dust on the spacecraft was correlated with illumination or material properties. The lunar surface, however, appeared undisturbed since the landing of Surveyor 3. Patterns made by the Surveyor 3 landing gear in the regolith appeared unchanged when the Apollo 12 astronauts visited. More dust measurements near the lunar surface are needed to assess the extent of charged dust movement.

The near-surface plasma environment, including the surface charge, determines the level of dust charge which in turn determines the ability of charged dust to levitate and be transported across the surface. A general picture of the global lunar surface potential has been constructed based on measurements and models of photoemission and of the solar wind (e.g., Manka 1973). Additional charging currents due to secondary electron emission when the Moon passes through the Earth's plasma sheet can enhance the surface charge. This has been indirectly measured by the Lunar Prospector, which detected electrons of moderate energy (~500 eV) ascending from the lunar nightside, suggesting a surface potential of up to ~500 V negative to accelerate the electrons to these energies (Halekas et al. 2005).

Experiments

The writers' previous experimental studies of charging and levitation of dust in a plasma sheath have been reported in Sickafoose

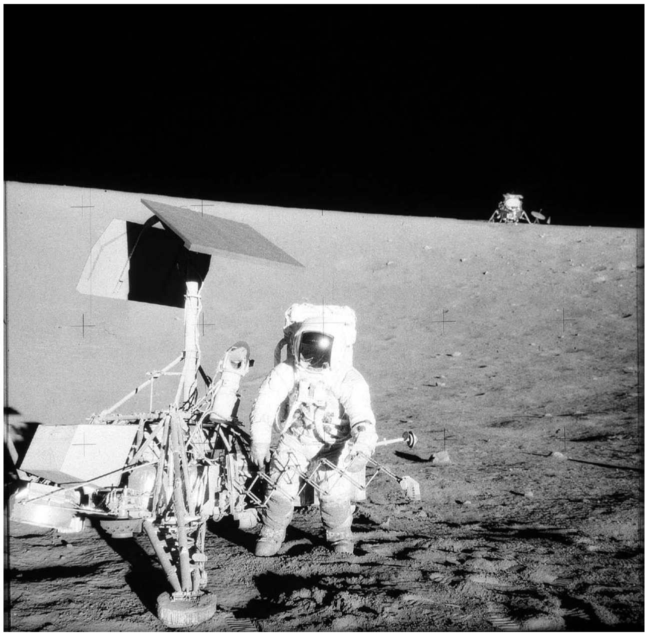

Fig. 2. Apollo 12 astronaut Charles "Pete" Conrad, Jr., near the Surveyor 3 spacecraft on the lunar surface on November 21, 1969, 31 months after Surveyor 3 landed. A small excavation of the lunar regolith is visible beneath the Surveyor spacecraft from its landing rocket. Some dust from the landing event made its way to the mirror in the television system, visible just to the left of Conrad's head in the image. The Apollo 12 Lunar Module is on the horizon 155 m away. Like the fine-patterned bootprints in the lunar regolith left by the astronauts, the Surveyor landing pads left detailed marks that were apparently undisturbed after 31 months. NASA photograph AS12-48-7136; Apollo 12 Principal Investigator, Dr. Richard J. Allenby, Jr.; National Space Science Data Center.

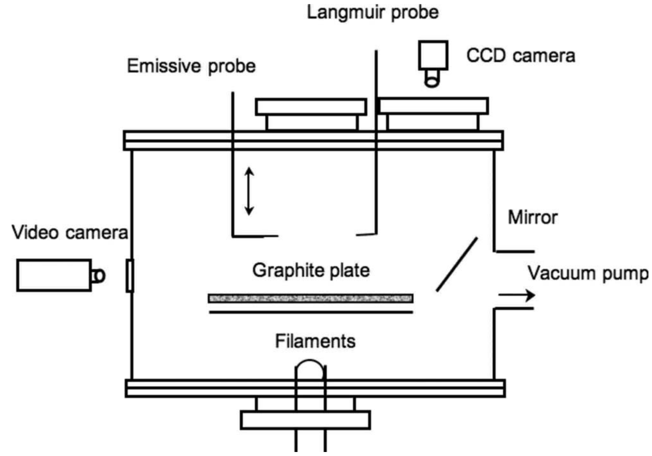

Fig. 3. Schematic diagram of plasma device configuration used for horizontal dust transport experiments and electric field measurements

et al. (2001, 2002), and Robertson et al. (2003). This paper presents the results of experimental studies of spreading of dust on a surface in a plasma. Although the experiments do not match the lunar surface conditions, they do allow the writers to verify their models of dust transport in a plasma sheath. The stainless steel plasma chamber is evacuated to a base pressure of 1.5×10^{-6} torr by a turbomolecular pump and the working pressure is 1.5×10^{-4} torr of argon. The plasma is generated by primary electrons from heated filaments biased to -40 V and emitting 350 mA. Dust samples are placed on a graphite plate 17.7 cm in diameter that is positioned approximately in the center of the vacuum chamber. This plate is electrically isolated and may be biased to a negative potential in the range -40 to -100 V. There is a 6 mm raised lip at the circumference of the plate to inhibit dust particles from moving past the edge. The experimental configuration is shown schematically in Fig. 3. The redistribution of dust on the surface is recorded by a charge-coupled device (CCD) still camera that views the graphite plate at an oblique angle. Individual particles are usually not resolved in these still images; they are used to map the redistribution of the initial pile or spot of particles on the surface. Dust floating above the surface is recorded by a CCD video camera aligned with the plate. Isolated individual particles can be tracked with the video camera. A second conducting plate below the graphite plate prevents heating of the graphite by the filaments and by the primary electrons from the filaments. The experiment is similar to that of Arnas et al. (1999, 2000) in which both the plate and the grains are charged by the primary electrons as well as by plasma electrons. In the writers' experiments, however, the conducting plate beneath the graphite plate prevents the primary electrons, which follow nearly straight trajectories, from contributing to the charging of dust grains on the upper surface of the graphite plate. The dust particles charge from the plasma currents, as they would on the lunar surface.

Plasma parameters are measured with a cylindrical Langmuir probe (wire diameter 0.30 mm and length 30 mm) located 80 mm above the graphite plate. The electron density is $n_e = 3-4 \times 10^7$ cm^{-3} and the electron temperature is 3.6–4.4 eV. The electrostatic potential $\Phi(r,z)$ is determined by an emissive probe like that described by Diebold et al. (1988). The emissive probe is mounted on a translation stage that is coupled to a data acquisition system so that potential measurements are made at 0.5 mm intervals. This probe may be mounted in either of two positions that allow scans to be made either vertically or horizontally. There is an uncertainty in the probe position of ± 2 mm due to flexure of the supports. The potential drop is concentrated in a sheath region within about 3 cm of the plate. The measured potential profiles are approximately those expected from the collisionless theory of the sheath (Robertson et al. 2003).

Here, JSC-Mars-1, a terrestrial analog to the Martian regolith, is used for horizontal dust transport experiments (Allen et al. 1998). Similar experiments have been done with the JSC-1 lunar regolith simulant, but the dark color of JSC-1 makes it difficult to get digitized measurements of the dust density on the dark graphite plate. Both JSC-Mars-1 and JSC-1 have low conductivities, and the writers' results with various conducting and nonconducting dust particles show that it is whether the particle is a conductor or insulator that determines the behavior of the dust near the surface. The dust is sieved to remove grains larger in size than 25 μm because the larger sizes are too massive to be levitated by the electric field (Sickafoose et al. 2002). A circular spot of dust $\sim$1 cm in diameter is placed on the plate with a thickness just sufficient to obscure the plate surface. There is sufficient contrast between the dust and the dark graphite plate to allow the dust to be clearly seen in images from the CCD camera.

In experiments where a small region of dust on a conducting surface is exposed to a plasma, nonconducting dust particles, such as lunar and Martian regolith simulants, spread horizontally. In previous experiments, a smooth diffusionlike spreading of the initial dust pile was found (Fig. 4). Further experiments show that

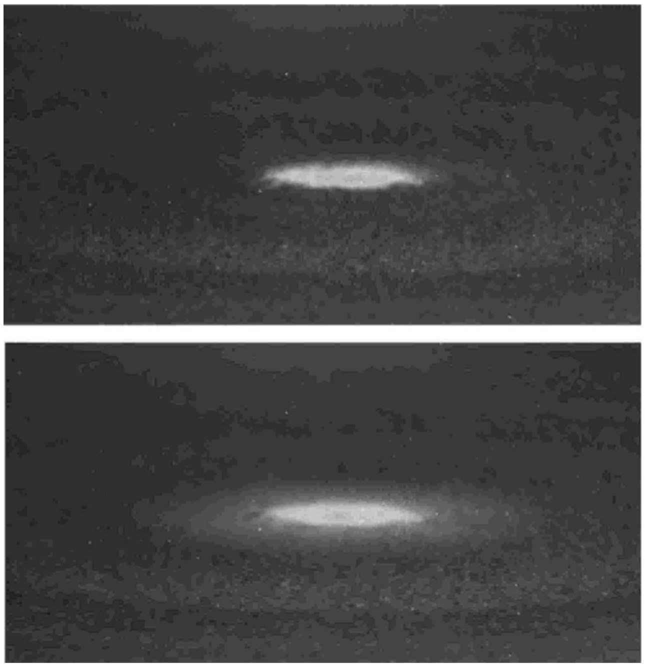

Fig. 4. Oblique views of JSC-Mars-1 dust on a graphite plate taken before (top) and after (bottom) the plasma was generated in the plasma device. A broad halo of dust surrounds the original dust spot location after only a few minutes exposure to plasma. The final distribution of dust is stable and no further spreading occurs.

the process is not diffusional. The spreading eventually stops. The final configuration of the dust is sensitive to the initial preparation of the dust spot. When particles are lightly sprinkled onto the surface into a thin pile, a more continuous final distribution (like that in Fig. 4) is produced. When the initial spot is thicker or particles are initially deposited by a brush rather than sprinkling on the graphite plate, an annulus of dust is created outside the initial spot as particles on the upper surface of the initial spot are transported away. Probe scans (described in the following) show that the dust particles charge to a potential that is significantly different from that of the conducting surface. This generates an electric field with a horizontal component that transports the dust away from the initial pile. The horizontal transport of dust stops in this case when the dust has been redistributed in such a way that the gradient in the potential is more smoothly varying so that the local electric field strength is too low for further transport.

Conducting dust on a conducting surface, on the other hand, remains at the same potential as the surface and no transport is observed. The difference in surface conductivities therefore leads to variations in the surface charge and the development of strong horizontal electric fields. Although this process is self-limiting in the plasma sheath experiments described, dust transport should occur via this process at the lunar terminator region. Photoemission of electrons from the illuminated surfaces leads to a higher effective conductivity than the adjacent shadowed regions. This has the same effect as the different material conductivities in the writers' experiments and produces electric fields capable of transporting dust.

To quantify the role of the electric field, the emissive probe was used to measure the potential profile above the dust. The emissive probe was mounted to be scanned horizontally at a nearly constant distance of 5 mm above the graphite plate. Data were noisy as a consequence of dust particles leaving the plate

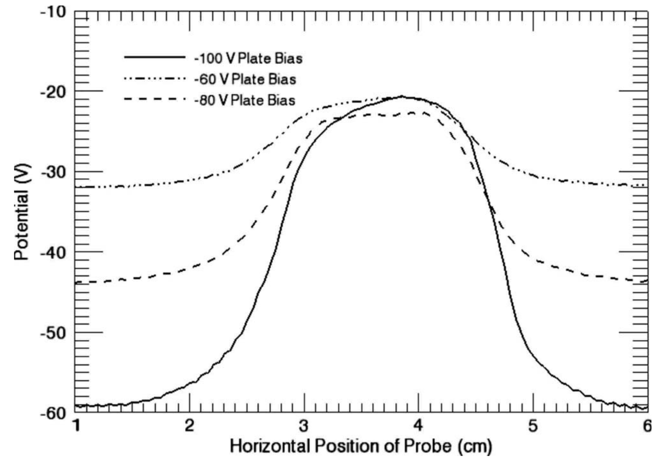

Fig. 5. Probe sweeps over an insulating glass disk on a graphite plate in a plasma sheath for graphite plate bias potentials of −60, −80, and −100 V. The sheath potential beyond the edges of the disk varies with the surface potential, but the insulating disk, a proxy for a layer of lunar dust, reaches the same potential regardless of the underlying surface potential.

and hitting the probe. To obtain less noisy data, the probe was scanned above a 12 mm diameter circular glass disk. The writers assume that the glass disk, being insulating, charges in the same way as the nonconducting dust. Scans above the glass disk show that the center of the disk remains near a constant potential of −22 V that is nearly independent of the potential applied to the graphite plate (Fig. 5). This potential is the floating potential of flat objects inserted into the plasma. Thus the horizontal potential gradient at the edge of the nonconductor depends upon the difference between the floating potential and the potential of the conducting plate. In these experiments, the biased plate is more negative than the nonconducting glass (or, equivalently, dust), thus the horizontal component of the electric field points radially outward. The measured horizontal electric field obtained by taking the derivative of the radial scans in Fig. 5 are shown in Fig. 6. The force is radially outward for positive particles; thus the particles that have moved outward are positively charged.

The positive charging of the particles on the surface can be explained as follows. For the present experiments, the floating potential of the graphite plate is −22 V at which the electron and ion currents to the plate are equal. The plate was always biased to a potential more negative than this, so the ion current density to the plate exceeds the electron current density and the dust particles on the plate collect more ions than electrons until the ion flux to the particle surface equals the electron flux. This results in a positive charge on the particles.

Numerical Simulations

In this paper, charged dust transport above the dayside lunar surface is modeled by calculating the trajectories of charged dust particles lifted off a dusty regolith, including gravitational and electrostatic forces as well as time-dependent charging of the particles. The charge, Q_d, is calculated from

$$\frac{dQ_d}{dt} = I_{\mathrm{pe}} - I_e - I_{\mathrm{sw}} \quad (1)$$

where the charging currents are due to photoemission from the grain (I_{pe}), collection of photoelectrons emitted from the lunar

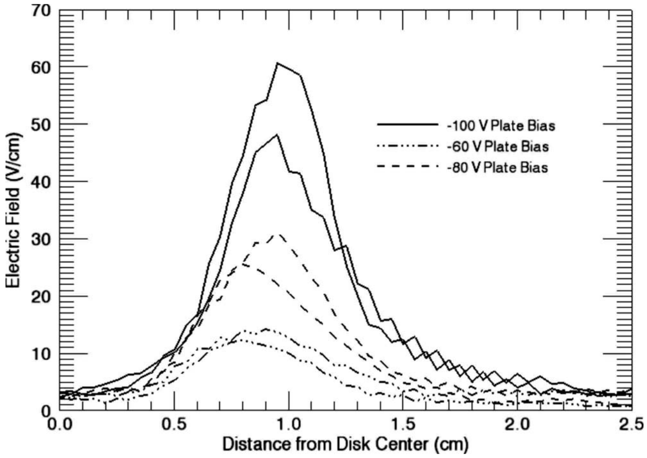

Fig. 6. Horizontal electric field determined by taking the derivative of the horizontal potential scans in Fig. 5. The electric field increases as the plate voltage increases and is positive, meaning the field is directed radially outward. The spreading of dust seen in Fig. 4 means the particles are positively charged.

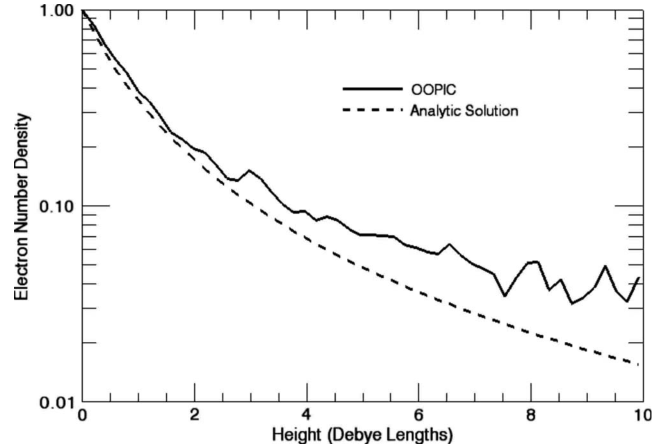

Fig. 7. Results from the OOPIC calculation for a photoelectron sheath with a Maxwellian electron velocity distribution and the analytic result from Grard and Tunaley (1971). The sheath electron densities have been normalized at the surface. The OOPIC result does not fall off as quickly as the analytic result is more than about 3 Debye lengths from the surface because of the counting statistics of small numbers of model electrons at those large distances from the surface. Calculations with more particles in the OOPIC simulation improve the agreement at large z.

surface (I_e), and collection of solar wind electrons (I_{sw}), respectively, and are given in Colwell et al. (2005) in terms of the local plasma properties. The solar wind ion current is negligible due to the positive charge attained by photoemission from the particle. In this simple model the writers also ignore time-variable currents from passage through the Earth's magnetotail. These currents are highly variable, and here the goal is to illustrate the possible charged-dust transport phenomenon in the standard dayside photoelectron layer. The one-dimensional particle trajectory is calculated by simultaneously solving the equation of motion

$$\frac{d^2z}{dt^2} = \frac{Q_d(t)}{m_d}E(z) - g \tag{2}$$

where $E(z)$=electric field resulting from the gradient in photoelectron density near the surface; m_d=mass of the particle; and g=local gravitational acceleration. Horizontal motion is assumed constant in these simulations, but the vertical electric field strength varies with position because the surface potential varies with local topography. These simulations do not yet model the experimental results presented in the previous section.

Both I_e in Eq. (1) and $E(z)$ depend on the vertical profile of the photoelectron layer, $n_{pe}(z)$. Assuming a simple velocity distribution for the photoelectrons emitted from the lunar surface it is possible to derive an analytic expression for n_{pe}. Grard and Tunaley (1971) derived profiles for monoenergetic, Heaviside, and Maxwellian electron energy distributions. A Maxwellian most closely resembles the expected electron energy distribution and gives a vertical photoelectron density of

$$n_{pe} = n_{pe,0}\left(1 + \frac{z}{\sqrt{2}\lambda_D}\right)^{-2} \tag{3}$$

where λ_D, the Debye length, depends on the mean photoelectron temperature. This temperature ($\sim$2.2 eV, Willis et al. 1973) in turn depends on the solar spectrum and the work function of the lunar surface. However, the solar spectrum at energies higher than the work function ($\sim$5 eV) is characterized by a rapidly decreasing flux with increasing energy punctuated by a few emission lines, most notably Lyman-α at 10.2 eV. Thus the energy spectrum of photons hitting the lunar surface that are capable of emitting electrons is not a blackbody spectrum, and the work function of the complex lunar regolith is not likely to be precisely the same value for all grains. The energy spectrum of the photoelectrons is therefore not likely to be exactly Maxwellian. Lacking an upper cutoff to the electron distribution, the photoelectron sheath described by Eq. (3) has infinite extent. In reality, the energies are limited and the sheath has a finite thickness.

To test the Grard and Tunaley model of the photoelectron layer, a particle-in-cell model was employed to compute the electron density above an electron-emitting plate. The commercial two-dimensional OOPIC Pro software was used, which models the plasma by discretizing time and space and calculating the positions and velocities of the plasma constituents at specific, discrete points in time and space. The code follows macroparticles which model individual electrons with particles with a larger mass and charge than a single electron. These model electrons are emitted from a circular plate with a mean energy of 4 eV. This is higher than the anticipated mean photoelectron energy from the lunar surface (2.2 eV), but the purpose of these calculations was to compare the OOPIC results with the analytic solution; so the precise energy values were not chosen to match any particular surface condition. The simulation space was made large enough so that boundary conditions did not influence the particles in the vicinity of the plate. The results of the OOPIC simulation with the analytic solution from Eq. (3) are shown in Fig. 7. The agreement is excellent within a few Debye lengths of the surface, and at greater distances from the surface the OOPIC approach predicts a higher electron number density. This comparison validates the OOPIC approach against a known analytic solution so that in future work the writers can use the OOPIC approach to test more realistic velocity distributions for which there are no analytic solutions to gauge their effect on the details of the photoelectron height profile.

The writers now use the analytic solution for the photoelectron sheath in numerical simulations of the trajectories of charged dust particles near the lunar surface. The model is based on the model applied to the asteroid Eros by Colwell et al. (2005), with solar wind, photoelectron emission, and gravity adjusted for lunar conditions. Because the numerical model of the sheath has no upper cutoff, the upward electric field, although weak, is present at all altitudes above the illuminated surface. This allows particles to reach a location where the electric force balances the gravitational force leading to stable levitation. With such a model, the electric field strength at some point above the surface is proportional to the potential produced by the photoemission current at the surface beneath that point. In shadowed regions of the present model, therefore, the electric field vanishes. This simplifies the actual three-dimensional behavior of the plasma near the surface at a shadow boundary, but over scales larger than a Debye length ($\sim$1 m), this transition region can be neglected. This also does not model the nightside electric field where solar wind plasma dominates the surface charge. The numerical results presented here are therefore applicable to shadows in craters $\geqslant$1 m, on the dayside, away from the global terminator. Any levitating dust moving over such a region would fall, leading to a net accumulation of dust in shadowed areas (Colwell et al. 2005). The size of particles that can stably levitate depends on the strength of the electric field, which in turn depends on the current of photoelectrons from the lunar surface.

The photoelectron current is determined by the flux of solar photons with sufficient energy to liberate electrons from the lunar regolith, $F(\lambda < \lambda_{\mathrm{crit}})$, and the quantum efficiency of photoemission from the material, $\chi(\lambda)$

$$I_{\mathrm{ph0}} = \int_0^{\lambda\mathrm{crit}} F(\lambda)\chi(\lambda)d\lambda \tag{4}$$

The longest wavelength photon that can produce a photoelectron is $\lambda_{\mathrm{crit}} \sim 250$ nm for a typical work function, W$\sim$5 eV (e.g., Sternovsky et al. 2002). The photoemission efficiency, $\chi(\lambda)$, is strongly wavelength dependent, and has been directly measured for lunar regolith samples taken by Apollo 14 and Apollo 15. The resulting photocurrent is $I_{\mathrm{ph0}}=2.8\times 10^9$ electrons/cm^2/s (Willis et al. 1973). The peak daytime photoelectron density at the surface is $n_{\mathrm{pe},0} \approx I_{\mathrm{ph0}}/\upsilon_{\mathrm{pe}}$, where υ_{pe}=characteristic photoelectron emission velocity of a few electron volts (e.g., Willis et al. 1973). This gives a photoelectron density at the surface of $n_{\mathrm{pe},0} \sim 60$ cm^{-3}, though this number is uncertain by at least a factor of a few due to uncertainties in I_{ph0} and the electron energy distribution, both of which may vary significantly with lunar soil type. Nevertheless, with these nominal values the photoelectron layer electric field strength is not strong enough to counter the lunar gravity for any particle size. Nitter and Havnes (1992) found electric fields capable of levitating submicron grains above the lunar surface in the solar wind plasma environment (not the dayside photoelectron layer).

The simulations in Fig. 8 were made with a photoemission current that was increased by factors of 5 and 10 to illustrate the phenomenon of charged dust levitation. The particles track the topography in the simulation. On bodies with weaker gravity, such as asteroids, levitation can occur with the nominal photoelectron flux. However, net transport of dust does not require this long-term stable levitation. The horizon glow observations as well as the LEAM measurements from the surface of the Moon can be explained by dust that is electrostatically launched off the surface but then follows a ballistic trajectory and reimpacts the surface a short distance away. Electrostatic launching can occur with the formation of strong local electric fields at shadow boundaries near the terminator. The different surface potentials between lit and unlit surface elements is analogous to the experiments with dielectric dust on a conducting plate described earlier. Depending on the local topography, some areas may have these strong local electric fields at terminator passages, whereas others do not. The resulting variations in illumination of the surface can therefore lead to areas that are able to have dust move under the electric force, whereas other areas act as a sink for this dust, leading to the same sort of net transport one gets with the stably levitating dust.

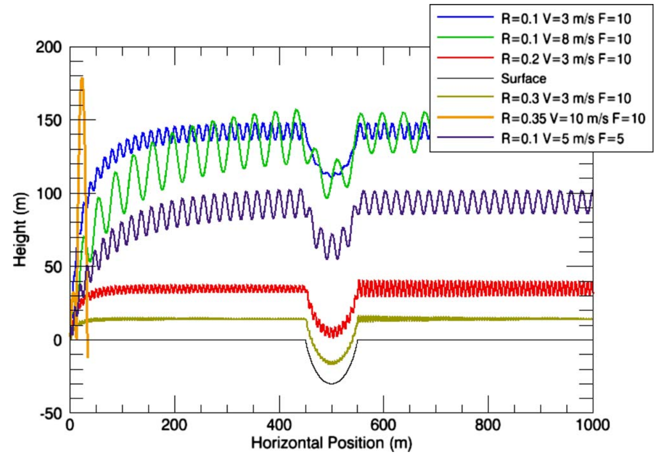

Fig. 8. Trajectories of particles knocked off the lunar surface at an 85° angle and at the indicated initial speeds at local noon at the equator on the Moon. "F" is the factor by which the nominal photoemission current (Colwell et al. 2005) has been increased to lead to stable levitation. The upward-pointing electric field generated in the near-surface photoelectron layer prevents the particle, which has a positive charge from its own photoemission above the photoelectron layer, from hitting the lunar surface. If the particle were to encounter the surface at a location where the electric field was weak or absent (such as a shadowed region, or an area with a higher work function), it would hit the surface at that location.

Discussion

Observations, though limited at the present time, suggest that charged dust movement near the lunar surface is most prominent near sunrise and sunset. The dawn/dusk asymmetry of the LEAM data is not understood by a simple terminator effect on local electric fields; however, the overall data set is limited and further observations are needed to explore the lunar horizon glow phenomenon. Theoretical expectations are for stronger local electric fields near the terminator (e.g., Borisov and Mall 2006), and this is consistent at least to first order with the observations currently available. Future observations will hopefully monitor both the local plasma environment as well as make in situ measurements of charged particles above the surface for extended durations (at least several lunar days) so that the dynamics of the dust can be related to the charging environment and surface potential.

Discussions of lunar horizon glow in the literature frequently refer to "levitation" of dust grains. There is an ambiguity in this term that has led to some confusion. Levitation may be taken to mean a stable long-term balance between the electric and gravitational force on a grain, such as depicted in Fig. 8. However, it has also been used to refer simply to the lifting of the particle off the surface, regardless of its subsequent dynamics. It is not possible to determine from the observations of the horizon glow whether the particles are stably levitating or are simply on modified ballistic trajectories above the surface. The astronaut observations of high altitude streaks may be submicron particles electrostatically launched from the surface and accelerated to high velocities (Stubbs et al. 2006). These particles would not be levitating in the sense of a stable layer. Here again, more observations are needed.

The experimental results presented here show that a net transport of charged dust can occur regardless of stable levitation if there is a gradient in the surface potential. In the writers' experiments this occurs with insulating dust on a conducting surface. The same phenomenon can occur with the lunar regolith at lit/shadowed boundaries. Surfaces exposed to sunlight become positively charged due to photoemission, whereas neighboring shadowed areas will be less positively charged. Small scale shadowed areas adjacent to directly illuminated areas occur near the terminator where the limited observations suggest that charged dust transport is most common.

Particles launched at low velocities into a photoelectron sheath charge negatively due to collection of photoelectrons and are quickly returned to the surface which is at a positive potential. The vertical scale of this negative charging region is roughly given by the sheath profile [Eq. (3)]. Particles launched slightly faster have enough momentum to carry them to higher altitudes where they can acquire a positive charge due to their own photoemission. These particles may become stably levitated or may simply reimpact the surface on nearly ballistic trajectories. There is a relatively narrow range of particle sizes and launch velocities that can lead to stable levitation in any sheath environment. If the surface gravity is low, such as on an asteroid, then particles may be accelerated to escape velocity instead of levitating (Lee 1996).

Even with the enhanced photoelectron current used in the writers' lunar simulations, it is found that only particles with a radius of $\sim 0.5\ \mu m$ and smaller can levitate above the lunar surface, whereas larger particles would follow nearly ballistic trajectories. For comparison, Rennilson and Criswell (1974) calculated a particle radius ten times larger for the source of the lunar horizon glow. This calculation assumes that the horizontal extent of the dust source of the observed glow is due to the light scattering properties of the particles and not any physical limitation on the cloud. Coupled with the writers' calculations and those of others (e.g., Borisov and Mall 2006), this suggests that the horizon glow particles are not stably levitating. The vertical extent of the cloud calculated by Rennilson and Criswell (1974) is only ~ 0.3 m, which corresponds to a vertical launch velocity of ~ 1 m/s. Experiments are currently under way to study the charge of individual particles on a surface in a plasma sheath, and these should shed light on the conditions that lead to particle separation from the surface and the velocity of those particles (Wang et al., 2006).

The charged dust dynamics above the lunar surface are certainly variable, but the amount of dust that moves in the near-surface plasma sheaths, and under what conditions, is unknown. Planned human activity on the lunar surface will be a much greater source of dust into the work environment than the natural process of charged dust levitation. Nevertheless, the dust kicked up by astronauts, rovers, and other equipment will be injected into a plasma environment that results in redistribution of dust that is contrary to terrestrial expectations and experience. Equipment deployed on the surface for extended periods may acquire a coating of fine-grained dust that can interfere with its operation. Different materials on lunar landers will charge to different floating potentials resulting in local electric fields that can affect the coating of equipment by dust. Whether there is significant stable levitation of particles, or if sporadic launching of grains from the surface onto ballistic trajectories dominates, lunar dust particles may be moving in all directions at the heights above the surface where exploration activities are planned to occur. Sunrise and sunset may be particularly active in terms of the Moon's dusty plasma weather. Measurements of the lunar plasma environment from a lunar lander would greatly improve the fidelity of models and simulations of the lunar dust environment so that future exploration activities on the lunar surface can be planned to minimize the dust hazard.

References

Allen, C. C., Jager, K. M., Morris, R. V., Lindstrom, D. J., Lindstrom, M. M., and Lockwood, J. P. (1998). "Martian soil simulant available for scientific, educational study." *EOS Trans. Am. Geophys. Union*, 79(34), 405.

Arnas, C., Mikikian, M., Bachet, G., and Doveil, F. (2000). "Sheath modification in the presence of dust particles." *Phys. Plasmas*, 7, 4418–4422.

Arnas, C., Mikikian, M., and Doveil, F. (1999). "High negative charge of a dust particle in a hot cathode discharge." *Phys. Rev. E*, 60, 7420–7425.

Bender, P. L., et al. (1973). "The Lunar laser ranging experiment." *Science*, 182, 229–238.

Berg, O. E., Richardson, F. F., and Burton, H. (1973). "Lunar ejecta and meteorites experiment." *Apollo 17 Prelimisary Science Rep. No. NASA SP-330*, Washington, D.C.

Berg, O. E., Wolf, H., and Rhee, J. (1976). "Lunar soil movement registered by the Apollo 17 cosmic dust experiment." *Interplanetary dust and zodiacal light*, H. Elsasser and H. Fechtig, eds., Springer, Heidelberg, Germany, 233–237.

Borisov, N., and Mall, U. (2006). "Charging and motion of dust grains near the terminator of the Moon." *Planet. Space Sci.*, 54, 572–580.

Colwell, J. E., Batiste, S., Horányi, M., Robertson, S., and Sture, S. (2007). "The lunar surface: Dust dynamics and regolith mechanics." *Rev. Geophys.*, 45, RG2006.

Colwell, J. E., Gulbis, A. A. S., Horányi, M., and Robertson, S. (2005). "Dust transport in photoelectron layers and the formation of dust ponds on Eros." *Icarus*, 175, 159–169.

Criswell, D. R. (1974). "Sunset intensification of lunar surface electric fields (abstract)." *Lunar interactions*, D. R. Criswell and J. R. Freeman, eds., The Lunar Science Institute, Houston, 100–102.

Criswell, D. R., and De, B. R. (1977). "Intense localized charging in the lunar sunset terminator region 2. Supercharging of at the progression of sunset." *J. Geophys. Res.*, 82(7), 1005–1007.

De, B. R., and Criswell, D. R. (1977). "Intense localized photoelectric charging in the lunar sunset terminator region 1. Development of potentials and fields." *J. Geophys. Res.*, 82(7), 999–1004.

Diebold, D., Hershkowitz, N., Bailey, A. D., III, Cho, M. H., and Intrator, T. (1988). "Emissive probe current bias method of measuring dc vacuum potential." *Rev. Sci. Instrum.*, 59, 270–275.

Doe, S. J., Burns, O., Pettit, D., Blacic, J., and Keaton, P. W. (1994). "The levitation of lunar dust via electrostatic forces." *Engineering, construction, and operations in space*, ASCE, New York, 907–915.

Grard, R. J. L., and Tunaley, J. K. E. (1971). "Photoelectron sheath near a planetary probe in interplanetary space." *J. Geophys. Res.*, 76, 2498–2505.

Halekas, J. S., Lin, R. P., and Mitchell, D. L. (2005). "Large negative lunar surface potentials in sunlight and shadow." *Geophys. Res. Lett.*, 32, L09102.

Lee, P. (1996). "Dust levitation on asteroids." *Icarus*, 124, 181–194.

Manka, R. H. (1973). "Plasma and potential at the lunar surface." *Photon and particle interactions with surfaces in space*, R. J. L. Grard, ed., Reidel, Dordrecht, The Netherlands, 347–361.

McCoy, J. E., and Criswell, D. R., (1974). "Evidence for a high altitude distribution of lunar dust." *Proc. 5th Lunar Conf.*, Vol. 3, Lunar and Planetary Institute, Houston, Tex., 2991–3005.

Nitter, T., and Havnes, O. (1992). "Dynamics of dust in a plasma sheath and injection of dust into the plasma sheath above the moon and asteroidal surfaces." *Earth, Moon, Planets*, 56, 7–34.

Nitter, T., Havnes, O., and Melandsø, F. (1998). "Levitation and dynamics of charged dust in the photoelectron sheath above surfaces in space." *J. Geophys. Res.*, 103, 6605–6620.

Pelizzari, M. A., and Criswell, D. R. (1978). "Lunar dust transport by photoelectric charging at sunset." *Proc., 9th Lunar Planet. Sci. Conf.*, 3225–3237.

Rennilson, J. J., and Criswell, D. R. (1974). "Surveyor observations of lunar horizon-glow." *Moon*, 10, 121–142.

Robertson, S., Gulbis, A. A. S., Colwell, J. E., and Horányi, M. (2003). "Dust grain charging and levitation in a weakly collisional sheath." *Phys. Plasmas*, 10, 3874–3880.

Sickafoose, A. A., Colwell, J. E., Horányi, M., and Robertson, S. (2000). "Photoelectric charging of dust particles in vacuum." *Phys. Rev. Lett.*, 84, 6034–6037.

Sickafoose, A. A., Colwell, J. E., Horányi, M., and Robertson, S. (2001). "Experimental investigations on photoelectric and triboelectric charging of dust." *J. Geophys. Res.*, 105, 8343–8356.

Sickafoose, A. A., Colwell, J. E., Horányi, M., and Robertson, S., (2002). "Experimental levitation of dust grains in a plasma sheath." *J. Geophys. Res.*, 107(A11), 1408.

Sternovsky, Z., Sickafoose, A. A., Colwell, J. E., Robertson, S., and Horányi, M. (2002). "Contact charging of lunar and Martian dust simulants." *J. Geophys. Res.*, 107(E11), 5105.

Stubbs, T. J., Vondrak, R. R., and Farrell, W. M. (2006). "A dynamic fountain model for lunar dust." *Adv. Space Res.*, 37, 59–66.

Wang, X, Colwell, J. E., Horányi, M., and Robertson, S. (2007). "Charge of dust on surfaces in plasma." *IEEE Trans. Plasma Sci.*, 35, 271–279

Willis, R. F., Anderegg, M., Feuerbacher, B., and Fitton, B. (1973). "Photoemission and secondary electron emission from lunar surface material." *Photon and particle interaction with surfaces in space*, R. J. L. Grard, ed., Reidel, Dordrecht, The Netherlands, 369–387.

Zook, H. A., and McCoy, J. E. (1991). "Large-scale lunar horizon glow and a high altitude lunar dust exosphere." *Geophys. Res. Lett.*, 18, 2117–2120.

Zook, H. A., Potter, A. E., and Cooper, B. L. (1995). "The lunar dust exosphere and Clementine lunar horizon glow." *Lunar Planet Science Conf.*, Vol. 26, 1577–1578.